Journal of Marine Science and Application (2025) 24: 1122-1140
https://doi.org/10.1007/s11804-025-00638-z

RESEARCH ARTICLE

Damage Detection of the Pipes Conveying Fluid on the Pasternak Foundation Using the Matching Pursuit Method

Nahid Khomarian[1], Ramazan-Ali Jafari-Talookolaei[1], Morteza Saadatmorad[1] and Reza Haghani[2]

Received: 02 October 2024 / Accepted: 21 November 2024

Abstract
The current study examines damage detection in fluid-conveying pipes supported on a Pasternak foundation. This study proposes a novel method that uses the matching pursuit (MP) algorithm for damage detection. The governing equations of motion for the pipe are derived using Hamilton's principle. The finite element method, combined with the Galerkin approach, is employed to obtain the mass, damping, and stiffness matrices. To identify damage locations through pipe mode-shape decomposition, an index called the "matching pursuit residual" is introduced as a novel contribution of this study. The proposed method facilitates damage detection at various levels and locations under different boundary conditions. The findings demonstrate that the MP residual damage index can accurately localize damage in the pipes. Furthermore, the results of the numerical and experimental tests showcase the efficiency of the proposed method, highlighting that the MP signal approximation algorithm effectively detects damage in structures.

Keywords Damage detection; Matching pursuit; Damaged pipe; Galerkin method; Finite element method

1 Introduction

Fluid-carrying pipes have varied applications in engineering fields and play a crucial role in transporting fluids such as oil, gas, and seawater (Wang, 2018). These pipes are often situated in challenging environments, such as offshore platforms, industrial plants, and urban infrastructure, where the risk of damage is significant. Therefore, understanding the dynamic behaviors of both intact and damaged fluid-conveying pipes is critical for ensuring their structural integrity and safe operation. This knowledge is particularly valuable to industries such as energy, petrochemicals, and civil engineering, where the prevention of pipeline failures can prevent costly downtime, environmental hazards, and safety risks. Additionally, developing effective damage detection methods (Song et al., 2018) can aid in proactive maintenance and extend the lifespan of these essential systems. Additionally, many structures are situated on foundations for which researchers used different mathematical models (Belabed et al., 2024; Bouafia et al., 2021; Ma et al., 2022; Lafi et al., 2024; Tounsi et al., 2024; Tounsi et al., 2023a; Tounsi et al., 2023b; Bounouara et al., 2023; Zaitoun et al., 2023; Tahir et al., 2022; Mudhaffar et al., 2023).

The investigation of vibrations in fluid-carrying pipes began in 1950 with the work of Ashley and Haviland (1950). The dynamic behaviors of these pipes were studied both theoretically (Benjamin, 1962) and experimentally (Benjamin, 1961). For example, Fu et al. (2023) investigated the nonlinear vibration analysis of viscoelastic axially functionally graded material pipes conveying pulsating internal flow. They found that elastic modulus, density, and coefficient of viscoelastic damping of the pipe material varied along the axial direction. They also used Euler–Bernoulli beam theory to model the transverse vibration equation of the viscoelastic axially functionally graded material pipe conveying pulsating fluid. Vassilev and Djoundjorov (2006) analyzed the dynamic stability of fluid-carrying pipes

Article Highlights

- This article demonstrates the effectiveness of the signal approximation method, matching pursuit, in detecting damage in pipes conveying fluid on the Pasternak foundation.
- The article introduces a novel damage index, the matching pursuit residual, which is obtained by subtracting the signals approximated using the matching pursuit method from the original vibration mode shape signals of the damaged pipes conveying fluid on the Pasternak foundation.
- Numerical and experimental results demonstrate that the signal reconstruction algorithm is suitable for vibration mode shape-based damage detection.

✉ Ramazan-Ali Jafari-Talookolaei
ramazanali@gmail.com

[1] School of Mechanical Engineering, Babol Noshirvani University of Technology, Shariati Av., 47148-71167, Babol, Mazandaran, Iran

[2] HiFIT LLC, Queens, New York 11432, USA

using the Galerkin method. Chellapilla and Simha (2007) employed the Fourier series and Galerkin method to study the critical velocity of fluid-carrying pipes on a foundation, examining the problem under three different boundary conditions. The interaction between the fluid and the pipe was explored using the finite element (FE) method (Olson and Jamison, 1997) and the spectral FE method (Lee and Oh, 2003; Lee and Park, 2006). Chu and Lin (1995) presented a general FE formulation employing cubic Hermite interpolation for the dynamic analysis of fluid transmission pipes, considering both shear deformation and rotary inertia. In their work, they considered the dynamic effect of the fluid as external distributed forces acting on the supporting pipe.

Liu et al. (2010) studied the effect of hydrostatic pressure on the vibration dispersion characteristics of fluid-shell coupled structures, considering fluid-loaded cylindrical shells and fluid-filled cylindrical shells. Zhang et al. (2002) investigated the application of three-dimensional (3D) linearized Euler equations and the theory of linearized tension in their research. In this study, an FE formulation based on 3D elasticity theory for the shell was presented, along with the linearized Euler equation for the fluid. Li et al. (2018) investigated the application of the Galerkin method to represent the dynamic response of a fluid-conveying pipe with laterally moving supports at both ends of the pipe. Li et al. (2015a) also examined the nonlinear dynamic behavior of a submerged beam with moving supports at both ends. They derived the equation of motion using a Newtonian approach, after which they added a mass coefficient for the fluid mass attached to the beams. To investigate the dynamic behavior and stability of a multi-mouth fluid transmission pipe, El-Sayed and El-Mongy (2019) presented a new formula based on the variable iteration method. Huang et al. (2010) obtained the natural frequency of fluid-structure interaction in a fluid transmission pipeline using the Reduced-Order-Element-Galerkin method, deriving the natural frequency equations for various boundary conditions. Li and Yang (2017) determined the critical flow velocity and frequency of a fluid transmission pipe using a new semi-analytical method, considering the effects of boundary conditions. Ma et al. (2023) developed the harmonic differential quadrature method to analyze the one-dimensional vibration of pipes conveying fluid under various boundary conditions. This method employed trigonometric functions to formulate the harmonic test function, and the weighting coefficients were calculated explicitly.

Using FE tools, Chatzopoulou et al. (2016) investigated the influence of rotational loading on the mechanical behavior of seamless steel pipes with thick walls in deep water. Ni et al. (2011) presented a semi-analytical method and differential transformation technique to analyze the free vibration of fluid transmission pipes with different boundary conditions. Using the Euler–Bernoulli beam model and the generalized integral transform method, Fu et al. (2024) analyzed the dynamic behavior of an axially functionally graded pipeline conveying gas–liquid two-phase flow. They found that the interactions between structures and fluids refer to the effects that fluids exert on structures, which can manifest through various forces. Such an interaction is often of significant interest to engineers and structural designers.

Meanwhile, Tijsseling (1996) conducted a review of the literature on transient phenomena in fluid-filled pipes by focusing on the history of fluid-structure interaction research in the time domain. Using the FE method, Zhai et al. (2011) obtained the governing equation of the fluid-carrying pipe considering fluid-structure interaction and the effect of shear deformation. To solve this equation, they employed a combination of the perturbation method with the Galerkin method. Li et al. (2015b) provided a broad overview of the literature on the dynamic analysis of fluid-filled pipe systems with a focus on fluid-structure interaction. They compared models and simulation algorithms of varying degrees of sophistication and discussed their range of applications.

The dynamics of fluid-carrying pipes were experimentally investigated by Jendrzejczyk and Chen (1985) under six different types of boundary conditions. Anand (2015) conducted an analytical study of the laminar flow of nanofluids in a circular tube immersed in an isothermal external fluid. Ghadirian et al. (2022) examined nonlinear free vibrations and stability of fluid transmission pipes made of composite materials. They derived the equations of motion for the system using Hamilton's extended principle for open systems based on Timoshenko's beam theory. Meanwhile, Song et al. (2018) used guided waves and conducted a series of experiments on damage detection in large-diameter pipes, both with and without liquid. In their study, two types of liquid–water and machine oil–were chosen to fill the pipes and assess the influence of the filler. Meenakumari et al. (2024) investigated the fluid-structure interaction phenomena of a submerged long flexible cylinder conveying two-phase slug flows, considering the geometric and hydrodynamic nonlinearities.

Li et al. (2023) proposed an FE model for analyzing flexible pipes with localized damage in the outer layers. The fundamental concepts of deep learning, including convolutional neural networks, were discussed by Jafari et al. (2020). Additionally, they introduced the use of deep learning methods for preventing pipeline damage through early detection. The results indicated that such an approach can identify damages in the early stages. Gresil et al. (2017) investigated the application of guided wave excitation and damage detection in composite pipes using piezoelectric sensors. They also examined the use of a guided wave-based structural health monitoring method using ultrasonic

guided waves. Furthermore, Buethe et al. (2013) presented an approach for structural health monitoring using guided waves in pipe structures, thereby addressing challenges in pattern recognition for damage detection. An algorithm for structural health monitoring of subsea pipeline systems was developed by Bao et al. (2013).

Structural health monitoring is a crucial process in structural engineering that helps prevent structural failure and reduces operational costs. In this regard, various methods for structural health monitoring have been proposed by researchers (Farrar and Worden, 2007). One of the most popular structural health monitoring methods is vibration-based damage detection, which has attracted researchers' attention due to its numerous advantages (Das et al., 2016; Peeters et al., 2001; Saadatmorad et al., 2021). An important advantage of vibration-based methods is their ability to provide global testing. These methods are also cost-effective. In vibration-based tests, the global data of the structure are obtained using numerical or experimental modal analysis. These data are then used in damage identification methods to determine the location and sometimes the severity of the damage (Hou and Xia, 2021; Doebling et al., 1998).

Generally, vibration-based damage detection methods are divided into two main categories: frequency-based damage and mode-shape-based damage detection methods (Khatir et al., 2021). Yang and Wang (2010) investigated the detection of structural damages using natural frequencies. In their work, they introduced an assurance criterion for the natural frequency vector to detect damages in an eight-story structure. By applying this criterion, they were able to successfully identify the location and severity of the damage with high accuracy. A new damage identification formula was introduced by Sotoudehnia et al. (2019). Similarly, Sha et al. (2019) proposed a new damage detection method based on changes in relative natural frequencies for detecting damages in beam structures. The effectiveness of the proposed method in identifying and quantifying damages in beams was demonstrated. To detect the location of damages in beam structures, Seguini et al. (2022) used natural frequencies as input for an artificial neural network. Saadatmorad et al. (2024b) applied the covariance of vibrational mode shape to the continuous wavelet transform to detect damages in beams that were reinforced with nanoparticles.

Furthermore, Pandey et al. (1991) used the derivative of the vibration mode shapes and the curvature of mode shapes for detecting damage in simply supported and cantilever beams. Their method demonstrated effective performance in detecting damages in beams. Wahab and De Roeck (1999) used the derivative of mode shapes in beam and bridge structures to detect damages. Their approach demonstrated high performance in numerical and experimental damage detection scenarios. In their study, Nguyen (2014) used a mode-shape analysis approach to detect cracks in beam structures, concluding that projections of the mode shapes on normal planes served as a good damage detection index. Saadatmorad et al. (2022) proposed a novel damage index called the "Pearson correlation function of mode shapes" to detect cracks in steel beams. Their experimental and numerical results demonstrated the method's effectiveness in identifying the scracks. Nahvi and Jabbari (2005) demonstrated that crack damages tended to disappear when they are located at mode-shape nodes; nevertheless, damage detection based on mode shapes can still be accomplished with high accuracy.

As shown in the literature, damage detection methods based on mode shapes are superior to those based on natural frequency. This is because mode shapes are generally more sensitive to local damage while detecting damage using natural frequencies requires acquiring data from multiple damaged states of the considered structure (Saadatmorad et al., 2024a; Carden and Fanning, 2004).

A review of published studies indicates that, despite the widespread applications of fluid-conveying pipes, damage detection in these structures has not yet been extensively explored. Therefore, the objective of the current study is to fill this research gap. The novelty of the present work lies in suggesting a signal reconstruction-based algorithm called "matching pursuit (MP)" for detecting damages in fluid-conveying pipes. Typically, this algorithm is employed to reconstruct the signal or its approximation. However, this article proposes a novel approach by using the residuals generated from the approximation as effective indicators for identifying damage and errors in the signal. The foundation of this paper rests on the principle that high-frequency components within the signal can be detected in the residuals produced by the optimal atom in the MP algorithm. Initially, we modeled pipe conveying fluid on a Pasternak foundation, and its kinetic and potential energies were obtained. Then, using Hamilton's principle, the governing differential equation for the pipe's deformation was derived. These equations were solved using the FE method, along with the Galerkin method. The computed results were compared with existing results to verify their validity. After this verification, a novel structural damage detection method based on the MP algorithm was proposed for detecting damages in fluid-conveying pipe structures. Finally, the effectiveness of the proposed damage detection method was evaluated numerically and experimentally.

2 Mathematical modeling

Consider the elastic pipe shown in Figure 1, which is placed on a Pasternak foundation. The pipe has a length L, an internal diameter d, an outer diameter D, Young's modulus E, and a second moment of area I. An incompressible

fluid with a constant velocity V flows inside the pipe. The elastic stiffness and shear layer stiffness of the Pasternak foundation are denoted by k_f and k_s, respectively. As shown in Figure 1, the origin of the coordinate system is located at the left end of the pipe.

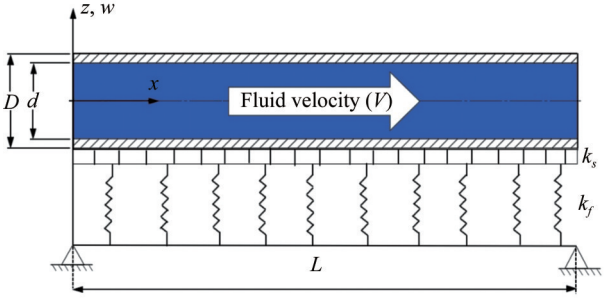

Figure 1 A schematic view of the pipe conveying fluid on the Pasternak foundation

The kinetic energy of the system consists of two parts that are related to the kinetic energy of the pipe and the fluid, respectively. The kinetic energy of the pipe can be expressed as follows:

$$T_p = \frac{1}{2}\rho_p A_p \int_0^L \left(\frac{\partial w(x,t)}{\partial t}\right)^2 \mathrm{d}x \tag{1}$$

The kinetic energy of the fluid is also calculated as follows:

$$T_f = \frac{1}{2}\rho_f A_f \int_0^L \left(\left(V\frac{\partial w(x,t)}{\partial x} + \frac{\partial w(x,t)}{\partial t}\right)^2 + V^2\right)\mathrm{d}x \tag{2}$$

In Eqs. (1) and (2), A and ρ are the area of cross-section and density, respectively; the subscripts p and f stand for the pipe and fluid, respectively; L is the length of the pipe; $w(x,t)$ represents the transverse displacement of the pipe at position x and time t; and V is the constant velocity of the fluid. Thus, the total kinetic energy of the system, which includes the kinetic energy of the pipe and the fluid, can be expressed as follows (Liang et al., 2018):

$$T = \frac{1}{2}\int_0^L \rho_p A_p \left(\frac{\partial w(x,t)}{\partial t}\right)^2 \mathrm{d}x + \frac{1}{2}\int_0^L \rho_f A_f \left(\left(V\frac{\partial w(x,t)}{\partial x} + \frac{\partial w(x,t)}{\partial t}\right)^2 + V^2\right)\mathrm{d}x \tag{3}$$

The strain energy of the pipe and foundation is expressed as follows (Yu et al., 2017; Jafari-Talookolaei and Ahmadian, 2007; Lee and Chung, 2002):

$$U = \frac{1}{2}\int_0^L EI\left(\frac{\partial^2 w}{\partial x^2}\right)^2 \mathrm{d}x + \frac{1}{2}\int_0^L \left(k_f w^2 + k_s\left(\frac{\partial w}{\partial x}\right)^2\right)\mathrm{d}x \tag{4}$$

The governing equation of motion for the free vibration of the considered tube was derived using Hamilton's principle as applied to a conservative system. The principle can be written as

$$\int_{t_1}^{t_2} (\delta T - \delta U)\,\mathrm{d}t = 0 \tag{5}$$

where t_1 and t_2 are two specified times, and δ denotes the first variation. Substituting Eqs. (3) and (4) into Eq. (5), and performing the first variation yields the following partial differential equation:

$$EIw_{,xxxx} + \rho_f A_f V^2 w_{,xx} + 2\rho_f A_f V w_{,xt} + \left(\rho_p A_p + \rho_f A_f\right) w_{,tt} + k_f w - k_s w_{,xx} = 0 \tag{6}$$

In this equation and in the following ones, a comma denotes differentiation with respect to the variable that immediately follows it.

3 Solution method

In the present work, the FE method was used, along with the Galerkin weighted residual method, to solve Eq. (6). A higher-order pipe element with length L_e, shown in Figure 2, was used in this study, which included two end nodes and one middle node. Each node contains two degrees of freedom of vertical displacement w and slope $w_{,x}$. Therefore, each element has six degrees of freedom. Thus, the degrees of freedom vector of an element are stated as follows:

$$\boldsymbol{d_e} = \left\{w_1, w_{1,x}, w_2, w_{2,x}, w_3, w_{3,x}\right\}^{\mathrm{T}} \tag{7}$$

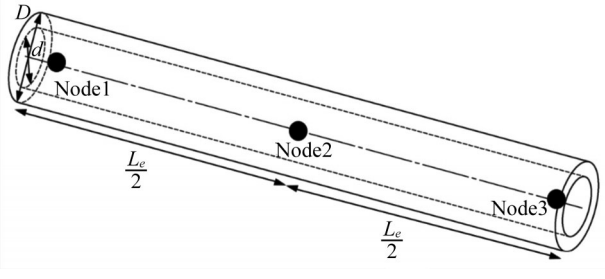

Figure 2 Higher-order pipe element used in the present study

The deflection of the pipe can be interpolated as follows:

$$w = \boldsymbol{N}\boldsymbol{d_e} \tag{8}$$

in which

$$\boldsymbol{N} = \begin{bmatrix} H_1 & \bar{H}_1 & H_2 & \bar{H}_2 & H_3 & \bar{H}_3 \end{bmatrix} \tag{9}$$

and H_i and $\bar{H}_i$ (i=1, 2, 3) are the Hermite interpolation functions (Logan, 2011). Based on the Galerkin method, we have (Logan, 2011) the following:

$$\iint RW\mathrm{d}x = 0 \tag{10}$$

where R is a weighted residual, and W is a weight function. Notably, for the Galerkin method used in the FE analysis, the weight function is the same as the shape function. By applying the Galerkin method to Eq. 6, we have the following:

$$\int_0^{L_e}\Big[EIw_{,xxxx} + \rho_f A_f V^2 w_{,xx} + 2\rho_f A_f V w_{,xt} + \left(\rho_p A_p + \rho_f A_f\right)w_{,tt} + k_f w + k_s w_{,xx}\Big]N_i L_e \mathrm{d}\xi = 0 \tag{11}$$

where $N_i = \left(H_1, \bar{H}_1, H_2, \bar{H}_2, H_3, \bar{H}_3\right)$. By using the integral by parts and writing the equations in weak form, the mass, damping, and stiffness matrices of an element can be calculated as follows:

$$\boldsymbol{M_e} = \left(\rho_p A_p + \rho_f A_f\right)\int_0^1 \boldsymbol{N}^{\mathrm{T}}\boldsymbol{N}L_e \mathrm{d}\xi \tag{12}$$

$$\boldsymbol{C_e} = \rho_f A_f V \int_0^1 \left(\boldsymbol{N}_{,x}^{\mathrm{T}}\boldsymbol{N} + \boldsymbol{N}^{\mathrm{T}}\boldsymbol{N}_{,x}\right)L_e \mathrm{d}\xi \tag{13}$$

$$\boldsymbol{K_e} = EI\int_0^1 \boldsymbol{N}_{,xx}^{\mathrm{T}}\boldsymbol{N}_{,xx}L_e \mathrm{d}\xi + \rho_f A_f V^2 \int_0^1 \boldsymbol{N}_{,x}^{\mathrm{T}}\boldsymbol{N}_{,x}L_e \mathrm{d}\xi + k_f\int_0^1 \boldsymbol{N}^{\mathrm{T}}\boldsymbol{N}L_e \mathrm{d}\xi + k_s\int_0^1 \boldsymbol{N}_{,x}^{\mathrm{T}}\boldsymbol{N}_{,x}L_e \mathrm{d}\xi \tag{14}$$

where $\xi = x/L_e$ represents the intrinsic coordinate of an element. Eventually, by assembling the equations of different elements, the final equations can be written in the following form:

$$\boldsymbol{M}\ddot{\Delta} + \boldsymbol{C}\dot{\Delta} + \boldsymbol{K}\Delta = 0 \tag{15}$$

where $\left(\boldsymbol{K}, \boldsymbol{C}, \boldsymbol{M}\right)$ are the total mass, damping, and stiffness matrices, respectively. Furthermore, $\left(\ddot{\Delta}, \dot{\Delta}, \Delta\right)$ are the acceleration, velocity, and degrees of freedom vectors of the pipe, respectively. The eigenvalues of the system can be computed by working out Eq. (15). Assuming the response to be in the form $\Delta = \underline{\Delta}\,\mathrm{e}^{\mathrm{i}\omega t}$ and substituting it into Eq. (15) and removing the term $\mathrm{e}^{\mathrm{i}\omega t}$, we will have the following:

$$\left(\boldsymbol{K} + \omega\boldsymbol{C} - \omega^2\boldsymbol{M}\right)\underline{\Delta} = 0 \tag{16}$$

in which i is the imaginary variable, $\underline{\Delta}$ is the amplitude of vibration, and ω is the frequency of the system. The above equation has been solved using MATLAB software, and the frequencies and mode shapes, i.e. $\underline{\Delta}$, have been calculated.

4 Methodology

In this study, a novel mode shape-based damage detection method is proposed, which uses the MP algorithm (Mallat and Zhang, 1993) to detect damages in the pipes conveying fluid on the Pasternak foundation. The MP algorithm is commonly used to approximate or reconstruct a signal. Notably, damage can be detected through the residual obtained from the difference between the original signal and the signal approximated or reconstructed by the MP algorithm. The probability of detecting damage in the residual obtained from the MP algorithm is high, because damage in the pipe conveying fluid manifests as a high-frequency disturbance that is not visible in the mode shapes. The flowchart of our proposed methodology is shown in Figure 3.

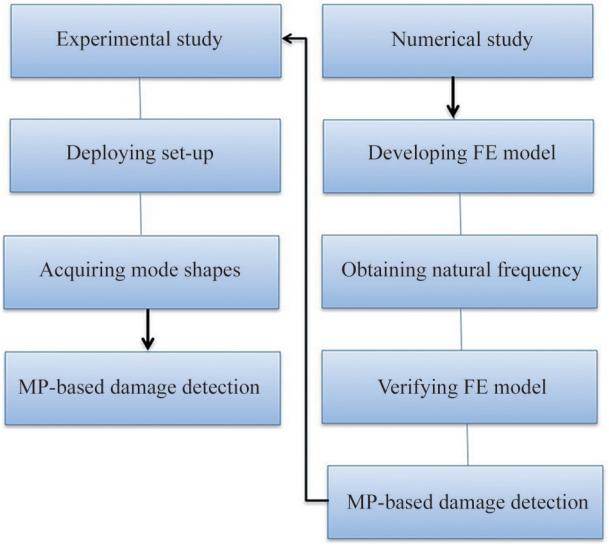

Figure 3 Flowchart of the proposed methodology of the current study

Consider a discrete signal $S[j]$ as follows (Mallat and Zhang, 1993; Chakraborty et al., 2009; Wang and Sun, 2019):

$$S[j] = \sum_{i=0}^{\infty}\alpha_i f_i[j] \tag{17}$$

where j is the sampling point number (node number), $f_i[j]$ is the basis function selected from the dictionary $\boldsymbol{D}$ at the ith iteration of the MP, and α_i is the corresponding expansion coefficient.

The energy of the signal can be represented by the following equation (Mallat and Zhang, 1993):

$$E_{[j]} = \left(\|S\|_2\right)^2 \triangleq \sum_{j=-\infty}^{+\infty}\left|S[j]\right|^2 \tag{18}$$

After n iterations, the result can be shown to converge as follows:

$$\lim_{n\to\infty}\left\| S[j]-\sum_{i=0}^{n-1}\alpha_i f_i[j]\right\|_2=0 \tag{19}$$

The signal can be defined using Eq. 20 (Mallat and Zhang, 1993):

$$S[j]=\sum_{i=0}^{n-1}\alpha_i f_i[j]+R_n[j] \tag{20}$$

where $R_n[j]$ is the residual signal after n iterations. The steps of the MP algorithm are presented as follows:

By setting $R_0[j]=S[j]$, in ith iteration, $i=0, 1, \cdots, n-1$, the residual $R_i[j]$ is computed on each dictionary atom $f^d[j]\in D$ until the following is obtained:

$$\Psi_i^{(d)}=\langle R_i, f^{(d)}\rangle \triangleq \sum_{-\infty}^{+\infty} R_i[j] f^{(d)}\times j\mathrm{d}j \tag{21}$$

The atom $f_i[j]$ selected from the dictionary is an atom that has the highest inner product value with the following residual:

$$f_i[j]=\operatorname{argmax}\left|\Psi_i^{(d)}\right| \tag{22}$$

The corresponding coefficients are written as follows (Mallat and Zhang, 1993):

$$\alpha_i=\langle R_i, f_i\rangle=\sum_{-\infty}^{+\infty} R_i[j] f_i[j]\mathrm{d}j \tag{23}$$

The residual in the (i+1)th iteration can be calculated as:

$$R_{i+1}[j]=R_i[j]-a_i f_i[j] \tag{24}$$

Thus, after n iterations of MP, the residual can be expressed as follows:

$$R_n[j]=R_{n-1}[j]-\alpha_{n-1}f_{n-1}[j]=S[j]-\sum_{i=0}^{n-1}\alpha_i f_i[j] \tag{25}$$

As shown in Table 1, the MP algorithm is a method to approximate a signal via a dictionary of functions. This algorithm operates iteratively to select the optimal function in the dictionary that best matches the residual signal at each step. The functions in the dictionary typically have waveforms. The most commonly used dictionaries are Gabor atoms, Fourier basis functions, and wavelet functions. At the first iteration, the first residual is the original signal. The algorithm iteratively selects the atom from the dictionary that is most similar to the current residual. This similarity is often measured using the inner product between the residual and each dictionary atom. The atom with the highest inner product is selected. After satisfying the stopping criterion, the final approximation of the signal is obtained by summing up all the selected atoms and their corresponding scaling coefficients.

Table 1 Matching pursuit algorithm

Inputs of MP: Signal: $S[j]$ Dictionary: $\boldsymbol{D}$
Output: List of coefficients $(a_i)_{i=1}^{n}$ and indices for corresponding atoms $\Psi_i^{(d)}$.
start:
$R_1=S[j]$; $i=1$;
Repeat:
Find $f_i[j]\in \boldsymbol{D}$ with maximum inner product $\left\lvert\langle R_i, f^d\rangle\right\rvert$;
$a_i=\langle R_i, f_i\rangle$;
$R_{i+1}=R_i-a_i f_{\psi_i}$;
$i=i+1$;
Stop condition (for example: $\lVert R_n\rVert <$ threshold)
Return

5 Weak matching pursuit

In the weak matching pursuit (WMP), the atom selection criterion is limited to a maximum value of inner multiplication less than one to have a computationally efficient method. This criterion is applied as follows:

$$\left\lvert\langle S, f_k\rangle\right\rvert \geqslant \beta \max\left\lvert\langle S, f_i\rangle\right\rvert, \quad \beta\in(0,1] \tag{26}$$

The MP for the weak condition is stated in Table 2.

Table 2 Weak matching pursuit algorithm

Inputs of MP: Signal: $S[j]$ Dictionary: $\boldsymbol{D}$
Output: List of coefficients $(a_i)_{i=1}^{n}$ and indices for corresponding atoms $\Psi_i^{(d)}$.
start:
$R_1=S[j]$; $i=1$;
Repeat:
Find $f_i[j]\in \boldsymbol{D}$ with maximum inner product $\left\lvert\langle R_i, f^d\rangle\right\rvert$;
While $\beta\in(0,1]$ do
β*max$\left\lvert\langle R_i, f_{\psi_i}\rangle\right\rvert$
$a_i=\langle R_i, f_i\rangle$;
$R_{i+1}=R_i-a_i f_i$;
$i=i+1$;
Stop condition (for example: $\lVert R_n\rVert <$ threshold)
Return

6 Results

The results of the current study are presented in this section. First, we verified the accuracy of the present modeling in Subsection 6.1. Then, in Subsection 6.2, we investigated numerical damage detection using six different numerical damage scenarios. After that, we analyzed the effect of noise on the damage indexes in Subsection 6.3. Finally, Subsection 6.4 presents the results of the experimental evaluations.

6.1 Comparison study

In this section, the calculated natural frequencies were compared with other references. We assume that the fluid velocity is zero. The natural frequencies are presented in dimensionless form. Here, results reported in three references (Liang et al., 2018; Ni et al., 2011; Thomson, 1993) were compared with the results of the present study. Table 3 shows the first four dimensionless natural frequencies $\left(\bar{\omega} = \frac{\omega L^2}{\sqrt{\frac{EI}{m_p + m_f}}}\right)$ of the tube with different boundary conditions and $V = 0$. As shown in this table, the results are in good agreement with the results reported in the literature (Liang et al., 2018; Ni et al., 2011; Thomson, 1993).

6.2 Numerical damage detection

In most studies, the MP algorithms aim to find the best-

Table 3 Dimensionless natural frequencies of pipes with different boundary conditions and $V = 0$

Boundary conditions	Method	Number of elements	$\bar{\omega}_1$	$\bar{\omega}_2$	$\bar{\omega}_3$	$\bar{\omega}_4$
Simple-Simple	Present	20	9.869	39.628	87.184	159.214
		25	9.869	39.628	87.186	159.211
		30	9.869	39.628	87.188	159.209
		35	9.869	39.628	87.188	159.208
		40	9.869	39.628	87.188	159.208
	Literature	Ni et al. (2011)	9.869	39.478	88.826	157.906
		Thomson (1993)	9.869	39.478	88.826	157.906
		Liang et al. (2018)	9.869	39.478	88.826	157.906
Clamped-Clamped	Present	20	22.373	62.014	122.195	200.308
		25	22.373	62.009	122.176	200.299
		30	22.373	62.014	122.195	200.308
		35	22.373	62.003	122.195	200.290
		40	22.373	62.003	122.195	200.290
	Literature	Ni et al. (2011)	22.373	61.672	120.903	199.840
		Thomson (1993)	22.373	61.672	120.903	199.840
		Liang et al. (2018)	22.373	61.672	120.903	199.840
Simple-Clamped	Present	20	15.418 2	50.128 6	105.162 7	167.802 2
		25	15.418	50.127 5	105.155 1	167.900 0
		30	15.418	50.126 8	105.149 6	167.966 6
		35	15.418	50.126	105.146	167.015
		40	15.418	50.126	105.146	167.015
	Literature	Ni et al. (2011)	15.418	49.964	104.247	178.264
		Thomson (1993)	15.418	49.964	104.247	178.264
		Liang et al. (2018)	15.418	49.964	104.247	178.264
Clamped-Free	Present	20	3.509	21.661	61.888	118.674
		25	3.511	21.658	61.917	118.650
		30	3.512	21.655	61.935	121.957
		35	3.513	21.654	61.948	121.977
		40	3.513	21.654	61.948	121.997
	Literature	Ni et al. (2011)	3.516	22.034	61.935	120.901
		Thomson (1993)	3.516	22.034	61.935	120.901
		Liang et al. (2018)	3.516	22.034	61.935	120.901

matched signal from the original signal. However, in the current study, our aim is to find the best residual using an MP algorithm to detect the location of damages in pipes carrying fluids. Thus, we used the mode shapes of a pipe with the properties listed in Table 4 to evaluate the numerical performance of the proposed MP algorithm. The mode shapes were obtained based on the FE modeling suggested in Section 2 and verified in subsection 3.1. In this method, the atom is the high-frequency component, and the residual represents the low-frequency component.

Table 4 Main properties of the considered pipe conveying fluid

Property	Symbol	Value
Total length of pipe (m)	L	10
Outer diameter (m)	D	0.25
Internal diameter (m)	d	0.125
Moment of area (m^4)	I	$\frac{\pi}{64}\left(D^4 - d^4\right)$
Area of the pipe (m^2)	A_p	$\frac{\pi}{4}\left(D^2 - d^2\right)$
Area of the fluid (m^2)	A_f	$\frac{\pi}{4d^2}$
Young's modulus (GN/m^2)	E	210
Density of pipe (kg/m^3)	ρ_p	8 700
Density of fluid (kg/m^3)	ρ_f	870
Mass of pipe (kg)	m_p	$\rho_p A_p L$
Mass of fluid (kg/m^3)	m_f	$\rho_f A_f$

The atom approximates the signal, and the damage locations are predicted in the residual. In other words, the proposed methodology suggests that instead of using MP for reconstructing the original signal, it can be used as a decomposition tool for damage detection. As shown in Table 5, 10 different damage scenarios are considered to examine the numerical performance of the proposed methodology.

The obtained mode shapes corresponding to the first six numerical damage scenarios are shown in Figure 4. As shown in the figure, detecting damages in most mode shapes is difficult or nearly impossible. Thus, we apply the proposed MP method. Figure 5 compares the damaged mode shapes with the approximation provided by the proposed MP method. Finally, Figure 6 indicates the residuals obtained from the proposed MP method. Evidently, the original signals (mode shapes) in all damage scenarios are well-fitted with the signals approximated by the MP method. This finding shows that the proposed method accurately processes the original signal. As shown in Figure 6, even at low damage percentages at different damage positions, the proposed MP method can accurately detect damage locations in the pipe as a break in the residual signals. Therefore, the suggested method is an effective numerical tool to identify the damages in the mode shapes of the pipe.

Figure 6 shows the results of damage detection for static fluid without the elastic foundation and Pasternak foundation. Furthermore, eight different damage scenarios with varying speeds and different values of k_s and k_f were considered to examine the numerical performance of the proposed methodology. The results are shown in Table 6.

As shown in Figure 7, the original signals in all damage scenarios are fitted with the signals approximated by the MP method. The approximated signals from the matching follow-up method are also shown. Figure 8 presents the residual signals and the results of damage detection. As shown in Figure 8, the proposed MP method can detect damage locations with high accuracy, even at low damage percentages at different damage positions.

As shown by the examined damage scenarios, the WMP algorithm can detect damages in all damage scenarios considered in Table 6 (for damages with different severities, in different positions, and with different boundary conditions of the pipe). In the next section, we investigated the effect of noise in the mode shape on the accuracy of damage identification with the proposed WMP.

Table 5 Ten damage scenarios considered in this study

Damage scenario	Damage location	Damage level	k_s (kN)	k_f (N/m^2)	V (m/s)	Boundary conditions
1	10	5%	0	0	0	Clamped-Clamped
2	20	3%	0	0	0	Simple-Clamped
3	76	1%	0	0	0	Clamped-Clamped
4	50	5%	0	0	0	Simple-Clamped
5	90	3%	0	0	0	Clamped-Clamped
6	42	1%	0	0	0	Simple-Clamped
7	90	3%	10^8	10^6	1.5	Clamped-Clamped
8	50	1%	0	0	1.5	Simple-Clamped
9	76	1%	0	10^6	0	Clamped-Clamped
10	20	3%	10^8	0	0	Simple-Clamped

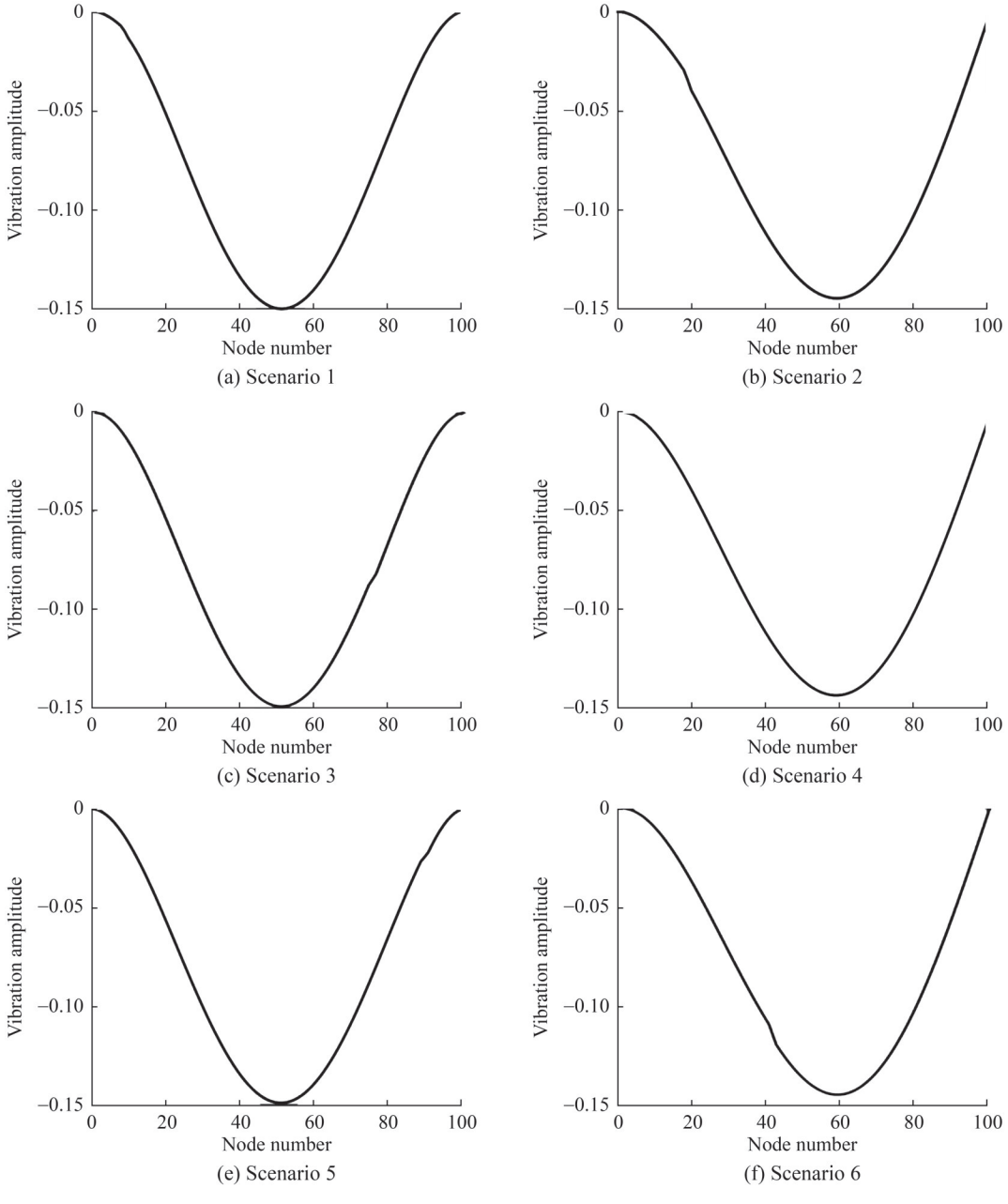

Figure 4 Damaged mode shapes for the considered damage scenarios ($V = 0, k_f = 0, k_s = 0$)

6.3 Effect of noise on the damage indexes

Due to the noises introduced in operational conditions, the performance of the proposed damage indicators in noisy conditions was examined in four separate scenarios in this section, as shown in Table 5 (Scenarios 7–10). Furthermore, the data were intentionally contaminated with random noise generated by MATLAB, with an intensity of 0.01%. The results obtained for Scenarios 7–10 are shown in Figures 9 and 10. In Figure 9, the original noisy signals in all damage scenarios are well-fitted with the signals approximated by the matching method. In Figure 10, we can see that despite the low damage level at different damage positions, the proposed MP method can detect the damage locations in the pipe as a break in the residual noise signals with high accuracy.

Figure 9 shows the quality of approximating the mode shapes related to Scenarios 7–10 by the WMP algorithm. The difference between these mode shapes and approximations created by the WMP algorithm is called the "residual", which we proposed as a damage identification index in this paper. The residuals corresponding to damage Scenarios 7–10 are shown in Figure 10. By comparing the results in Figures 9 and 10, we can see that the better the approximation of the signal, the higher the accuracy of damage identification in the residuals.

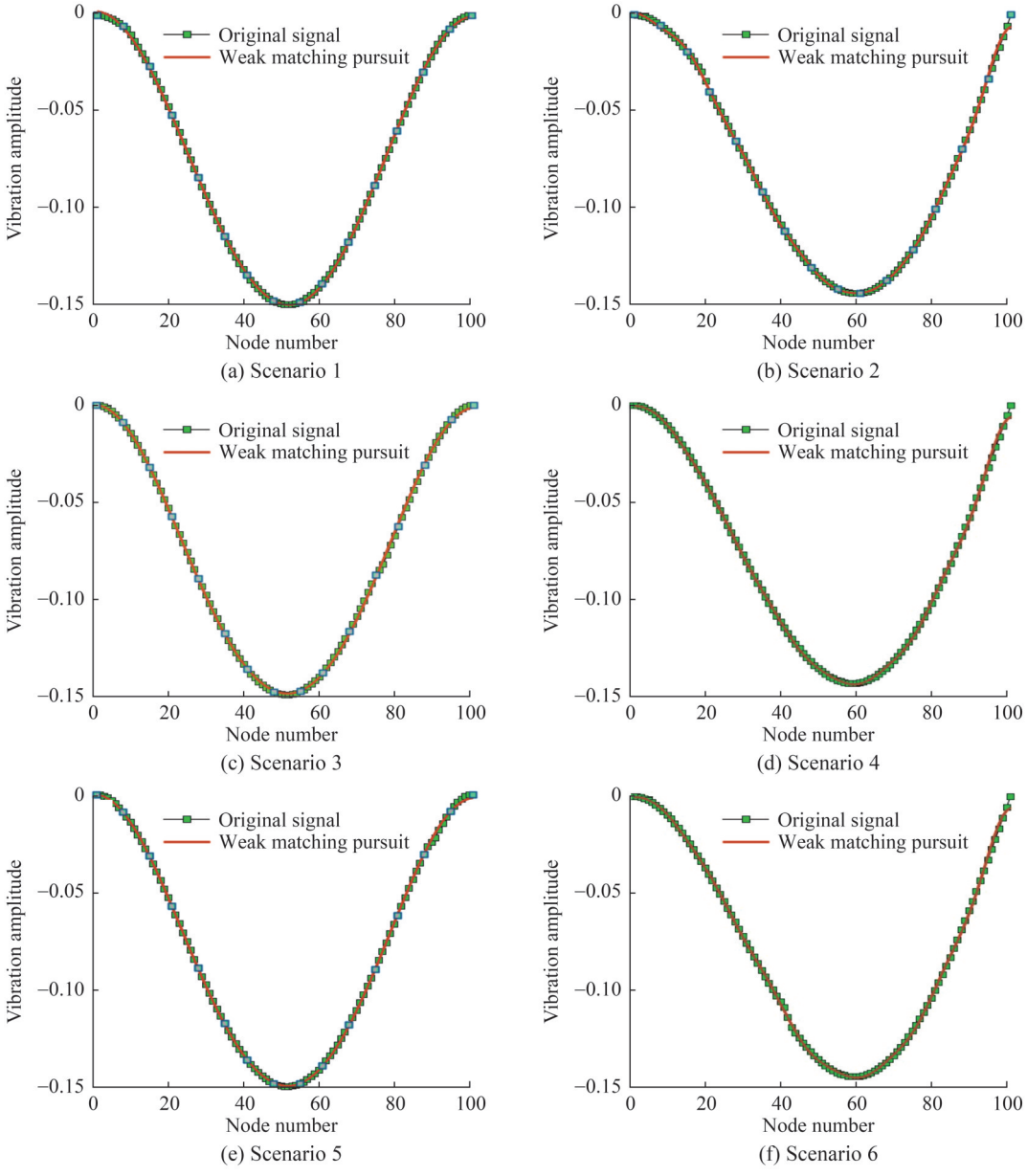

Figure 5 Comparison of the original signal and the signal approximated using the WPM algorithm ($V = 0, k_f = 0, k_s = 0$)

6.4 Experimental damage detection

In this section, we validated the method presented in operational conditions using modal testing. Figure 11 shows the steps of measuring and applying damage on the steel 304 pipe for the modal test. To conduct the modal test, the pipe-carrying fluid was suspended using two soft strings. As shown in Figure 12, the pipe was divided into 20 segments. Next, to measure acceleration, two one-way piezoelectric accelerometers were installed at points 3 and 12 of the structure. The accelerometer remained fixed at both points. A modal impact hammer equipped with a force gauge was used to apply force to the structure, which was done at all points by moving the hammer along the pipe. Subsequently, the analyzer was used to calculate the force and acceleration signals and obtain the frequency response functions.

Figure 13 shows the laboratory equipment and the test setup, while Figure 14 presents the experimental setup and its different components.

Finally, the obtained frequency response functions were analyzed. The natural frequencies and damping coefficients are reported in Table 7.

The data for the normalized mode shapes of the steel 304 pipe carrying water are presented in Table 7. Eventually, we tested our proposed damage detection methodology for localizing damage in the pipe with the experimental first mode shape. Figure 15 compares the original signal and

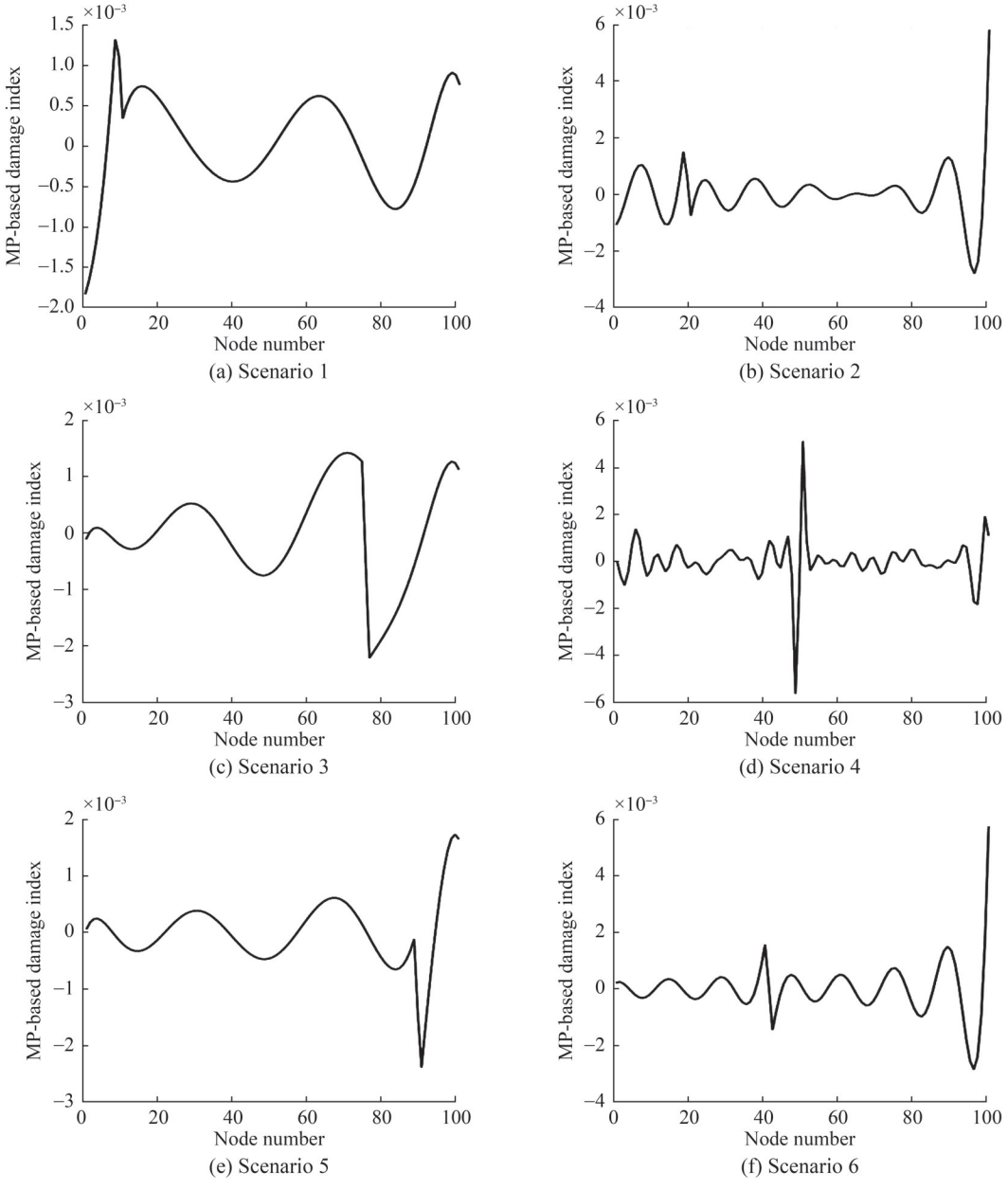

Figure 6 The residual signals obtained from the WPM algorithm and results of damage detection ($V = 0, k_f = 0, k_s = 0$)

Table 6 Eight damage scenarios considered in this study

Damage scenario	Damage location	Damage level	k_s (kN)	k_f (N/m^2)	V (m/s)	Boundary conditions
1	90	3%	10^8	0	0	Simple-Clamped
2	76	1%	10^6	0	0	Clamped-Clamped
3	20	3%	0	10^4	0	Simple-Clamped
4	76	1%	0	10^6	0	Clamped-Clamped
5	90	3%	0	0	1.5	Clamped-Clamped
6	42	1%	0	0	3	Simple-Clamped
7	90	3%	10^8	10^6	1.5	Clamped-Clamped
8	20	3%	10^{10}	10^4	0.3	Simple-Clamped

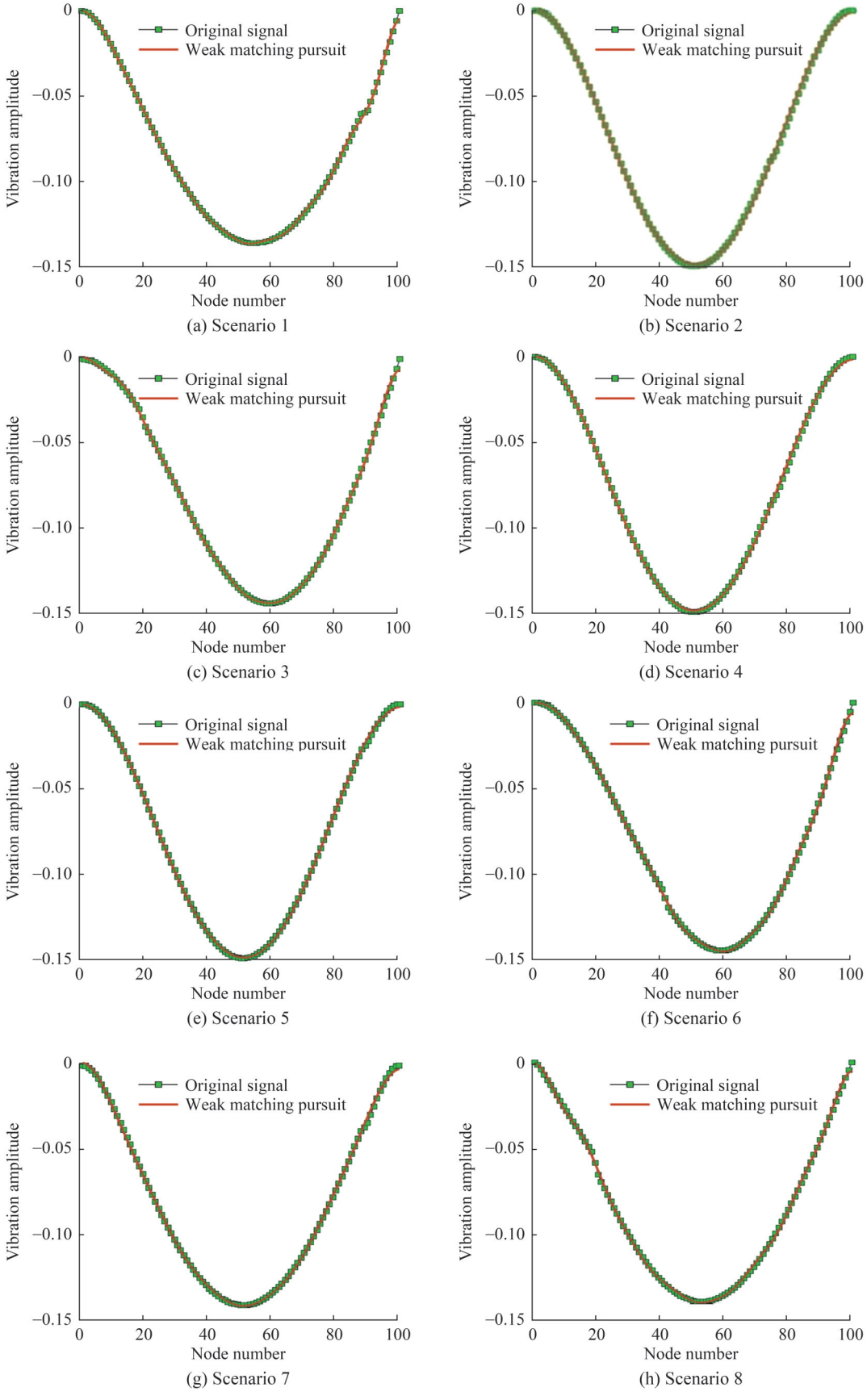

Figure 7 Comparison of the original signal and the signal approximated using the WPM algorithm

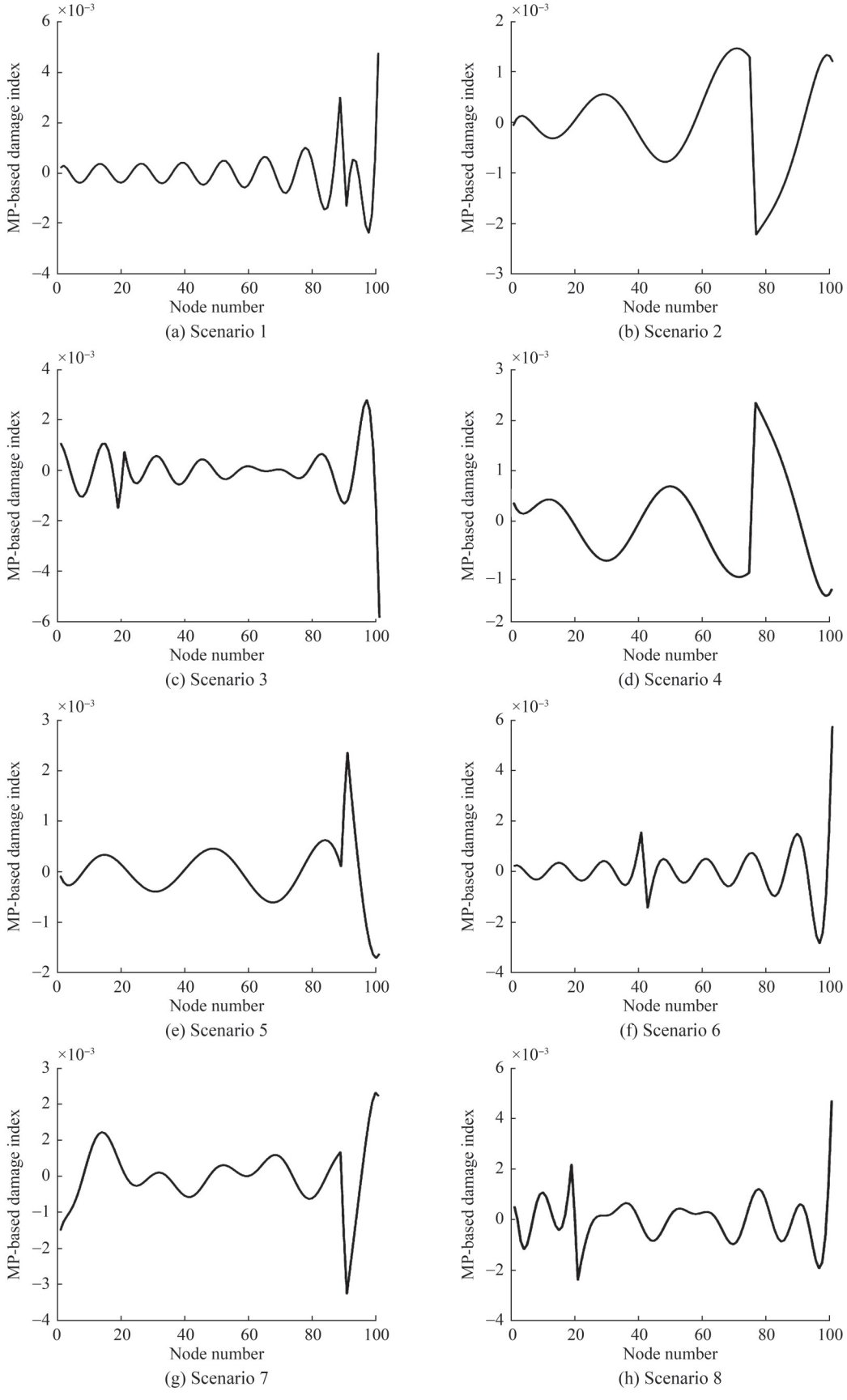

Figure 8 The residual signals obtained from the WPM algorithm and the results of damage detection

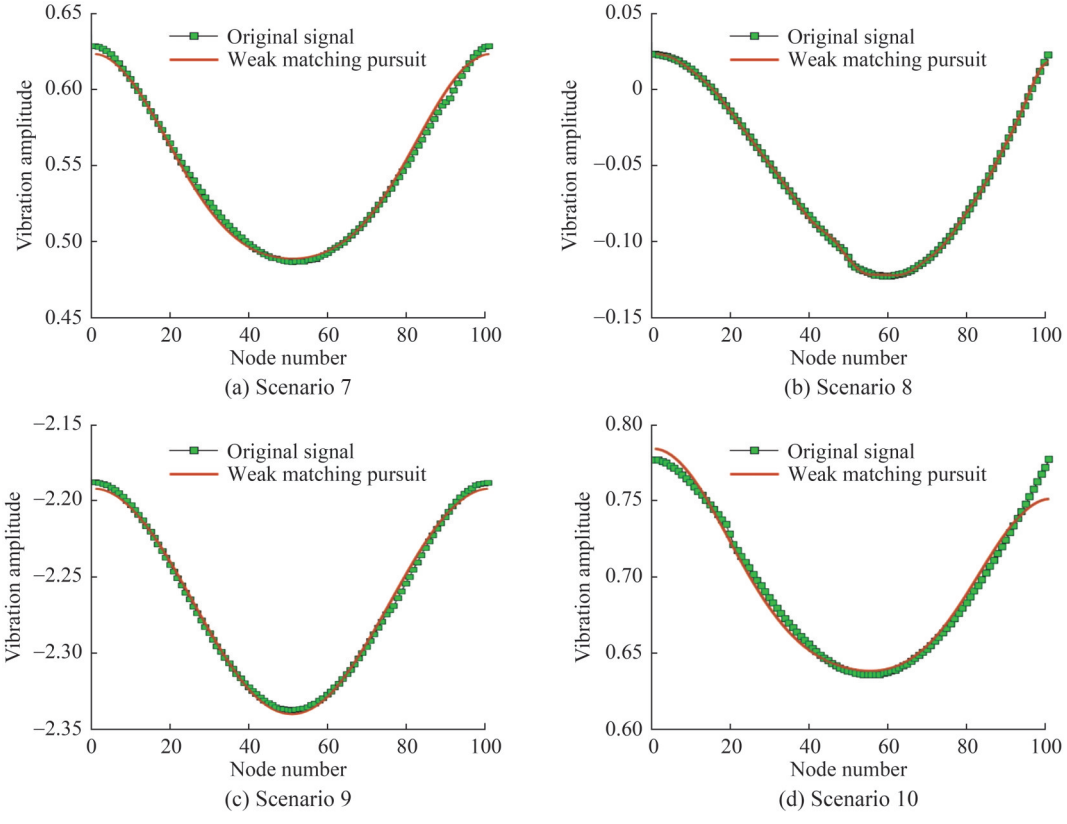

Figure 9 Comparison of the noisy original signal and the signal approximated using the WPM algorithm

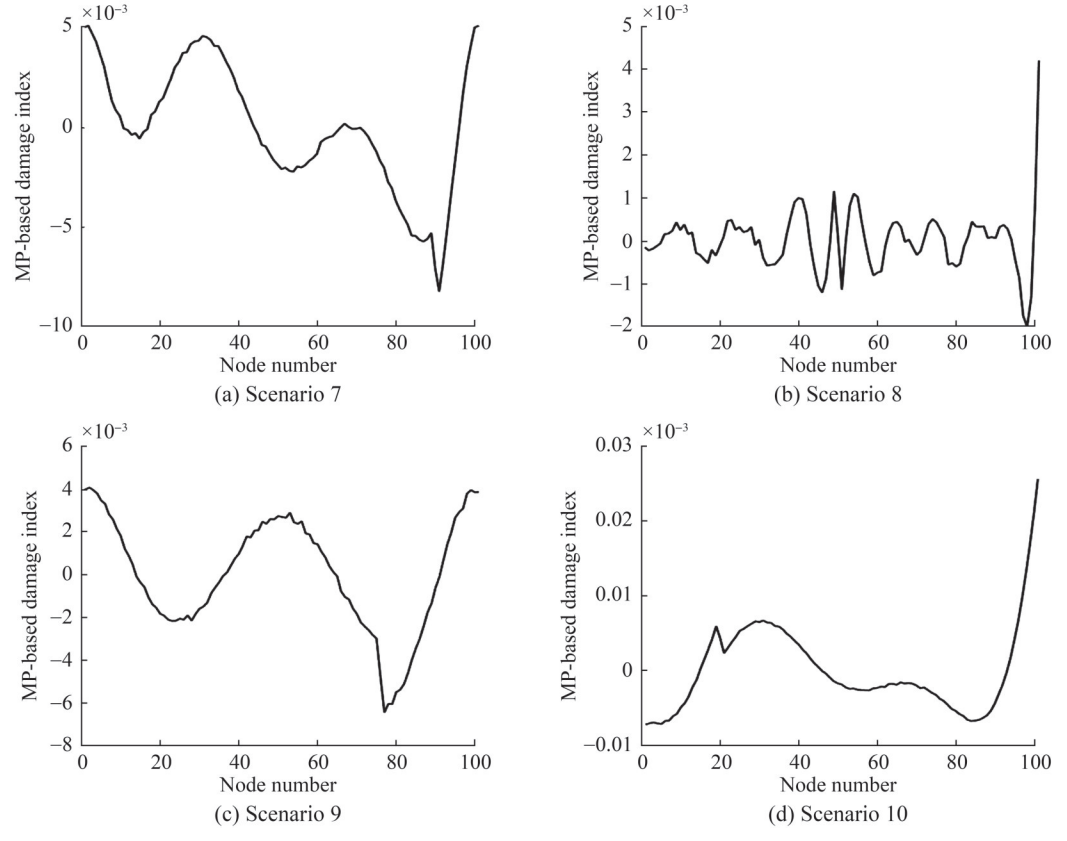

Figure 10 Residual noisy signals obtained from the WPM algorithm and the results of damage detection

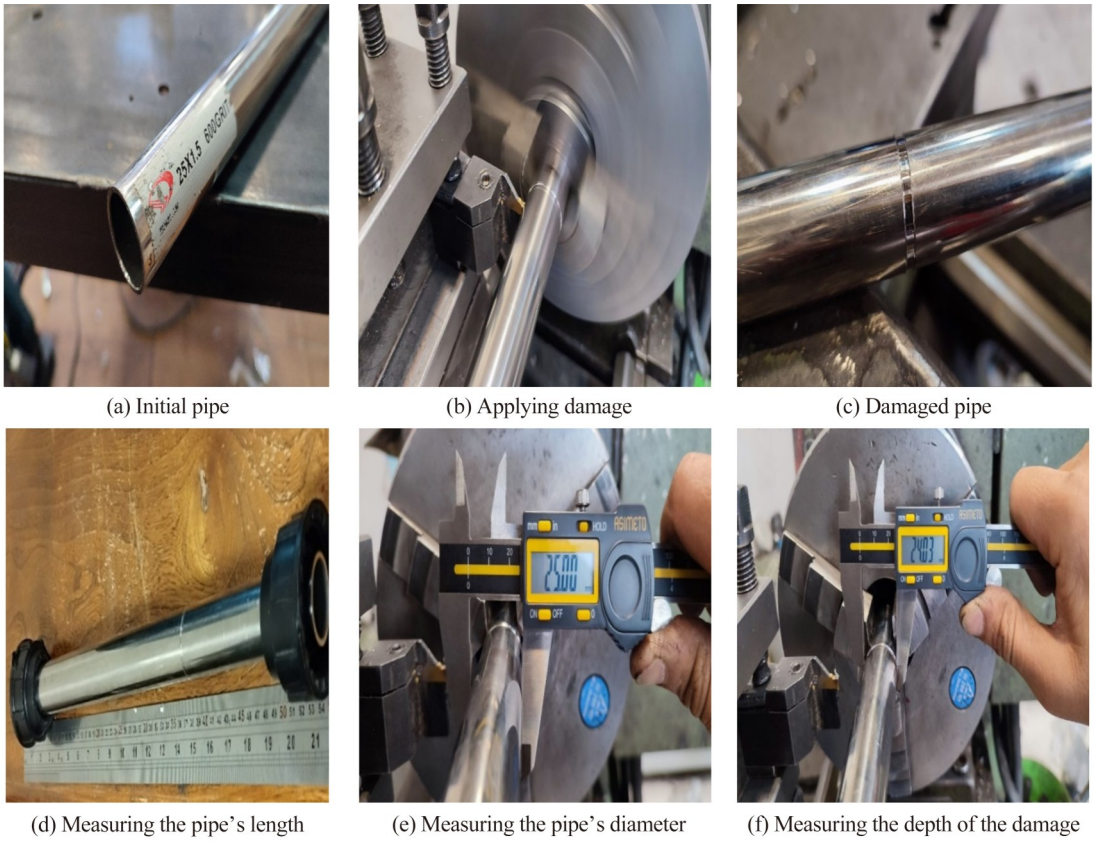

Figure 11 Steps of applying damage and measuring the pipe

Figure 12 Meshing the pipe and displaying the damage location

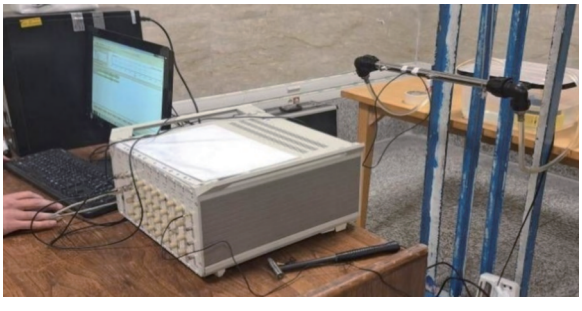

Figure 13 Experimental modal analysis: pipe conveying fluid and equipment for data acquisition system and the modal impact hammer

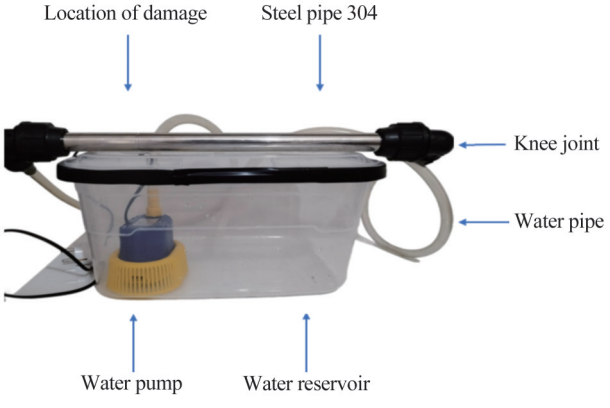

Figure 14 Test setup and its different components

Table 7 Natural frequencies and damping coefficients of steel pipe carrying fluid

Mode number	1	2	3
Natural frequency (Hz)	662.20	1 295.90	2 362.41
Damping ratio	4.74	2.13	1.94

the approximated signal using the weak MP tracking algorithm. Figure 16 shows the residual obtained from the proposed MP method. As can be seen, the original signal (first mode shape) is well-fitted with the signal approximated by the proposed MP method. This shows that the proposed method processes the original signal correctly. Furthermore, as seen in Figure 16, the proposed MP algorithm detects the location of damage with high accuracy, even with few experimental sampling data.

Table 8 Normalized mode shapes of the steel pipe carrying fluid

Node number	Mode 1	Mode 2	Mode 3
1	−0.267 0	−0.563 5	0.367 6
2	−0.254 6	0.596 0	0.125 0
3	−0.142 3	0.131 4	0.133 5
4	−0.105 7	0.203 8	0.710 1
5	−0.352 6	0.276 5	0.215 6
6	0.724 6	0.319 0	0.995 1
7	0.131 8	0.423 5	0.514 3
8	0.182 1	0.286 4	−0.732 9
9	0.241 1	0.158 0	−0.980 5
10	0.313 9	0.117 1	−0.414 8
11	0.313 4	0.113 7	−0.407 4
12	0.362 3	−0.105 8	−0.118 3
13	0.319 3	−0.159 8	−0.721 2
14	0.304 5	−0.236 3	−0.614 6
15	0.268 1	−0.242 0	0.218 8
16	0.226 1	−0.286 1	0.118 0
17	0.182 6	−0.303 1	0.307 9
18	0.104 3	−0.271 6	0.148 9
19	−0.325 2	−0.161 0	0.389 1
20	−0.107 9	−0.327 9	0.425 0

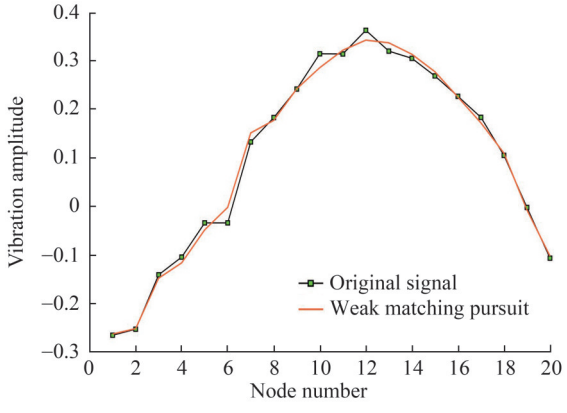

Figure 15 Comparison of the original signal and approximated signal using the weak matching tracking algorithm

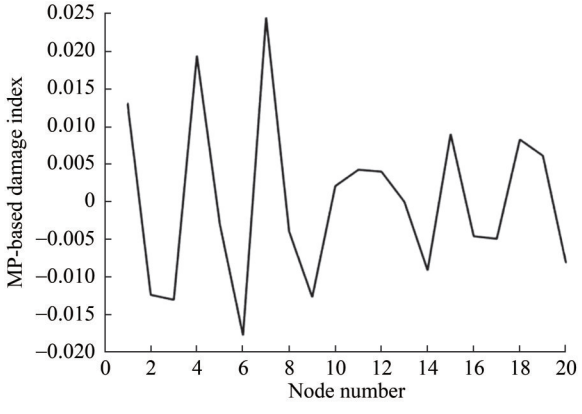

Figure 16 Residual signal obtained from the WMP algorithm and damage detection results

7 Conclusions

In this study, numerical and experimental approaches were presented to identify damage in fluid-conveying pipes, which are critical components in various engineering applications, such as oil and gas transportation, water supply systems, and chemical processing. Maintaining the structural integrity of these pipes is crucial, because any damage can result in leaks, reduced efficiency, and catastrophic failures. The dynamic behavior of fluid-conveying pipes is influenced by several factors, including pipe material properties, fluid flow velocity, and external support conditions, such as those provided by a Pasternak foundation. In this study, the governing equation for the pipe supported by a Pasternak foundation is derived based on the Euler–Bernoulli beam theory, and the response is calculated using the finite element method.

This study introduces the potential of a signal approximation algorithm called the MP method for detecting damage and demonstrates its efficacy in accurately locating damage under varying conditions. The damage index proposed in this study is based on the difference between the mode shape of the pipe structure and the approximation signal obtained from the MP algorithm (i. e., the residual signal). This innovative approach enhances traditional damage detection methods by providing a more sensitive and reliable method of monitoring pipe integrity.

Our findings reveal that the MP algorithm effectively identifies damage regardless of boundary conditions, varying damage intensities, and the proximity of damage to support. Given the widespread use of fluid-carrying pipes across various industries, ensuring reliable damage detection in these structures is critical. In the current study, the combination of theoretical modeling and experimental validation enhanced the credibility of the results, making it a robust tool for engineers and researchers in the field. Furthermore, this study provides a robust foundation for future research, serving as a benchmark for further investigations into the dynamic behavior of fluid-carrying pipes and the application of the MP algorithm for signal analysis and damage detection.

Competing interest The authors have no competing interests to declare that are relevant to the content of this article.

References

Anand V (2015) Entropy generation analysis of laminar flow of a nanofluid in a circular tube immersed in an isothermal external fluid. Energ. 93: 154-164. https://doi.org/10.1016/j.energy.2015.09.019

Ashley H, Haviland G (1950) Bending vibrations of a pipe line containing flowing fluid. J. Appl. Mech. 17(3): 229-232. https://doi.org/10.1115/1.4010447

Bao C, Hao H, Li ZX (2013) Integrated ARMA model method for damage detection of subsea pipeline system. Eng. Struct. 48: 176-192. https://doi.org/10.1016/j.engstruct.2012.09.033

Belabed Z, Tounsi A, Al-Osta MA, Tounsi A, Minh HL (2024) On the elastic stability and free vibration responses of functionally graded porous beams resting on Winkler-Pasternak foundations via finite element computation. Geomech. & Eng. 36(2): 183. https://doi.org/10.12989/gae.2024.36.2.183

Benjamin TB (1962) Dynamics of a system of articulated pipes conveying fluid-I. Theory. Proc. R. Soc. Lond. A 261(1307): 457-486. https://doi.org/10.1098/rspa.1961.0090

Benjamin TB, Batchelor GK (1961) Dynamics of a system of articulated pipes conveying fluid-II. Experiments. Proc. R. Soc. Lond. A 261(1307): 487-499. https://doi.org/10.1098/rspa.1961.0091

Bouafia K, Selim MM, Bourada F, Bousahla AA, Bourada M, Tounsi A, Tounsi A (2021) Bending and free vibration characteristics of various compositions of FG plates on elastic foundation via quasi 3D HSDT model. Steel & Compos. Struct. 41(4): 487-503. https://doi.org/10.12989/scs.2021.41.4.487

Bounouara F, Sadoun M, Saleh MMS, Chikh A, Bousahla AA, Kaci A, Bourada F, Tounsi A, Tounsi A (2023) Effect of visco-Pasternak foundation on thermo-mechanical bending response of anisotropic thick laminated composite plates. Steel Compos. Struct. 47(6): 693-707. https://doi.org/10.12989/scs.2023.47.6.693

Buethe I, Torres-Arredondo MA, Mujica Delgado LE, Rodellar Benedé J, Fritzen CP (2013) Damage detection in piping systems using pattern recognition techniques. In Proceedings 6th European Workshop on Structural Health Monitoring & 1st European Conference on Prognostics and Health Management, Dresden, Germany, 1-8

Carden EP, Fanning P (2004) Vibration based condition monitoring: a review. Struct. Healt. Monit. 3(4): 355-377. https://doi.org/10.1177/1475921704047500

Chakraborty D, Kovvali N, Wei J, Papandreou-Suppappola A, Cochran D, Chattopadhyay A (2009) Damage classification structural health monitoring in bolted structures using time-frequency techniques. J. Intell. Mater. Sys. & Struct. 20(11): 1289-1305. https://doi.org/10.1177/1045389X08100044

Chatzopoulou G, Karamanos SA, Varelis GE (2016) Finite element analysis of cyclically-loaded steel pipes during deep water reeling installation. Ocean Eng. 124: 113-124 https://doi.org/10.1016/j.oceaneng.2016.07.048

Chellapilla KR, Simha HS (2007) Critical velocity of fluid-conveying pipes resting on two-parameter foundation. J. Sound Vib. 302(1-2): 387-397. https://doi.org/10.1016/j.jsv.2006.11.007

Chu CL, Lin YH (1995) Finite element analysis of fluid - conveying timoshenko pipes. Shock Vib. 2(3): 247-255. https://doi.org/10.3233/SAV-1995-2306

Das S, Saha P, Patro SK (2016) Vibration-based damage detection techniques used for health monitoring of structures: a review. J. Civ. Struct. Health Monit. 6: 477-507. https://doi.org/10.1007/s13349-016-0168-5

Doebling SW, Farrar CR, Prime MB (1998) A summary review of vibration-based damage identification methods. Shock Vib. Digest 30(2): 91-105. https://doi.org/10.1177/058310249803000201

El-Sayed TA, El-Mongy HH (2019) Free vibration and stability analysis of a multi-span pipe conveying fluid using exact and variational iteration methods combined with transfer matrix method. Appl. Math. Model. 71: 173-193. https://doi.org/10.1016/j.apm.2019.02.006

Farrar CR, Worden K (2007) An introduction to structural health monitoring. Phil. Trans. R. Soc. A. 365(1851): 303-315. https://doi.org/10.1098/rsta.2006.1928

Fu G, Tuo Y, Zhang H, Su J, Sun B, Wang K, Lou M (2023) Effects of material characteristics on nonlinear dynamics of viscoelastic axially functionally graded material pipe conveying pulsating fluid. J. Mar. Sci. Technol. 22: 247-259. https://doi.org/10.1007/s11804-023-00328-8

Fu G, Wang X, Wang B, Su J, Wang K, Sun B (2024) Dynamic behavior of axially functionally graded pipe conveying gas–liquid two-phase flow. Appl. Ocean Res. 142: 103827. https://doi.org/10.1016/j.apor.2023.103827

Ghadirian H, Mohebpour S, Malekzadeh P, Daneshmand F (2022) Nonlinear free vibrations and stability analysis of FG-CNTRC pipes conveying fluid based on Timoshenko model. Compos. Struct. 292: 115637. https://doi.org/10.1016/j.compstruct.2022.115637

Gresil M, Poohsai A, Chandarana N (2017) Guided wave propagation and damage detection in composite pipes using piezoelectric sensors. Procedia. Eng. 188: 148-155. https://doi.org/10.1016/j.proeng.2017.04.468

Hou R, Xia Y (2021) Review on the new development of vibration-based damage identification for civil engineering structures: 2010-2019. J. Sound Vib. 491: 115741. https://doi.org/10.1016/j.jsv.2020.115741

Huang YM, Liu YS, Li BH, Li YJ, Yue ZF (2010) Natural frequency analysis of fluid conveying pipeline with different boundary conditions. Nucl. Eng. Des. 240(3): 461-467. https://doi.org/10.1016/j.nucengdes.2009.11.038

Jafari R, Razvarz S, Gegov A, Vatchova B (2020) Deep learning for pipeline damage detection: an overview of the concepts and a survey of the state-of-the-art. In 2020 IEEE 10th International Conference on Intelligent Systems, 178-182. https://doi.org/10.1109/IS48319.2020.9200137

Jafari-Talookolaei RA, Ahmadian MT (2007) Free vibration analysis of a cross-ply laminated composite beam on pasternak foundation. J. Comput. Sci. 3(1): 51-56. https://doi.org/10.3844/jcssp.2007.51.56

Jendrzejczyk JA, Chen SS (1985) Experiments on tubes conveying fluid. Thin-Walled Struct. 3(2): 109-134. https://doi.org/10.1016/0263-8231(85)90028-X

Khatir S, Tiachacht S, Le Thanh C, Tran-Ngoc H, Mirjalili S, Wahab MA (2021) A new robust flexibility index for structural damage identification and quantification. Eng. Fail. Anal. 129: 105714. https://doi.org/10.1016/j.engfailanal.2021.105714

Lafi DE, Bouhadra A, Mamen B, Menasria A, Bourada M, Bousahla AA, Bourada F, Tounsi A, Tounsi A, Yaylaci M (2024) Combined influence of variable distribution models and boundary conditions on the thermodynamic behavior of FG sandwich plates lying on various elastic foundations. Struct. Eng. Mech. 89(2): 103-119. https://doi.org/10.12989/sem.2024.89.2.103

Lee SI, Chung J (2002) New non-linear modelling for vibration analysis of a straight pipe conveying fluid. J. Sound Vib. 254(2): 313-325. https://doi.org/10.1006/jsvi.2001.4097

Lee U, Oh H (2003) The spectral element model for pipelines conveying internal steady flow. Eng. Struct. 25(8): 1045-1055. https://doi.org/10.1016/S0141-0296(03)00047-6

Lee U, Park J (2006) Spectral element modelling and analysis of a pipeline conveying internal unsteady fluid. J. Fluids Struct. 22(2): 273-292. https://doi.org/10.1016/j.jfluidstructs.2005.09.003

Li B, Wang Z, Jing L (2018) Dynamic response of pipe conveying fluid with lateral moving supports. Shock Vib. 2018(1): 3295787. https://doi.org/10.1155/2018/3295787

Li M, Ni Q, Wang L (2015a) Nonlinear dynamics of an underwater slender beam with two axially moving supports. Ocean Eng. 108: 402-415. https://doi.org/10.1016/j.oceaneng.2015.08.015

Li S, Karney BW, Liu G (2015b) FSI research in pipeline systems–A review of the literature. J. Fluids Struct. 57: 277-297. https://doi.org/10.1016/j.jfluidstructs.2015.06.020

Li X, Vaz MA, Custódio AB (2023) A finite element methodology for birdcaging analysis of flexible pipes with damaged outer layers. Mar. Struct. 89: 103397. https://doi.org/10.1016/j.marstruc.2023.103397

Li YD, Yang YR (2017) Vibration analysis of conveying fluid pipe via He's variational iteration method. Appl. Math. Model. 43: 409-420. https://doi.org/10.1016/j.apm.2016.11.029

Liang X, Zha X, Jiang X, Wang L, Leng J, Cao Z (2018) Semi-analytical solution for dynamic behavior of a fluid-conveying pipe with different boundary conditions. Ocean Eng. 163: 183-190. https://doi.org/10.1016/j.oceaneng.2018.05.060

Liu ZZ, Li TY, Zhu X, Zhang JJ (2010) The effect of hydrostatic pressure fields on the dispersion characteristics of fluid-shell coupled system. J. Mar. Sci. 9: 129-136. https://doi.org/10.1007/s11804-010-9010-3

Logan DL (2011) A first course in the finite element method. 4th edn, Thomson, Canada

Ma Y, You Y, Chen K, Feng A (2022) Analysis of vibration stability of fluid conveying pipe on the two-parameter foundation with elastic support boundary conditions. J. Ocean Eng. Sci. 9(6):616-629. https://doi.org/10.1016/j.joes.2022.11.002

Ma Y, You Y, Chen K, Hu L, Feng A (2023) Application of harmonic differential quadrature (HDQ) method for vibration analysis of pipes conveying fluid. Appl. Math. Comput. 439: 127613. https://doi.org/10.1016/j.amc.2022.127613

Mallat SG, Zhang Z (1993) Matching pursuits with time-frequency dictionaries. IEEE Trans. Signal Process. 41(12): 3397-3415. https://doi.org/10.1109/78.258082

Meenakumari HNR, Zanganeh H, Hossain M (2024) Effect of slug characteristics on the nonlinear dynamic response of a long flexible fluid-conveying cylinder. Appl. Ocean Res.147: 103978. https://doi.org/10.1016/j.apor.2024.103978

Mudhaffar IM, Chikh A, Tounsi A, Al-Osta MA, Al-Zahrani MM, Al-Dulaijan SU (2023) Impact of viscoelastic foundation on bending behavior of FG plate subjected to hygro-thermo-mechanical loads. Struct. Eng. Mech. 86(2): 167-180. https://doi.org/10.12989/sem.2023.86.2.167

Nahvi H, Jabbari M (2005) Crack detection in beams using experimental modal data and finite element model. Int. J. Mech. Sci. 47(10): 1477-1497. https://doi.org/10.1016/j.ijmecsci.2005.06.008

Nguyen KV (2014) Mode shapes analysis of a cracked beam and its application for crack detection. J. Sound Vib. 333(3): 848-872. https://doi.org/10.1016/j.jsv.2013.10.006

Ni Q, Zhang ZL, Wang L (2011) Application of the differential transformation method to vibration analysis of pipes conveying fluid. Appl. Math. Comput. 217(16): 7028-7038. https://doi.org/10.1016/j.amc.2011.01.116

Olson LG, Jamison D (1997) Application of a general purpose finite element method to elastic pipes conveying fluid. J. Fluids Struct. 11(2): 207-222. https://doi.org/10.1006/jfls.1996.0073

Pandey AK, Biswas M, Samman MM (1991) Damage detection from changes in curvature mode shapes. J. Sound Vib. 145(2): 321-332. https://doi.org/10.1016/0022-460X(91)90595-B

Peeters B, Maeck J, De Roeck G (2001) Vibration-based damage detection in civil engineering: excitation sources and temperature effects. Smart Mater. Struct. 10(3): 518. https://doi.org/10.1088/0964-1726/10/3/314

Saadatmorad M, Jafari-Talookolaei RA, Pashaei MH, Khatir S (2021) Damage detection on rectangular laminated composite plates using wavelet based convolutional neural network technique. Compos. Struct. 278: 114656. https://doi.org/10.1016/j.compstruct.2021.114656

Saadatmorad M, Khatir S, Cuong-Le T, Benaissa B, Mahmoudi S (2024a) Detecting damages in metallic beam structures using a novel wavelet selection criterion. J. Sound Vib. 578: 118297. https://doi.org/10.1016/j.jsv.2024.118297

Saadatmorad M, Shahavi MH, Gholipour A (2024b) Damage detection in laminated composite beams reinforced with nano-particles using covariance of vibration mode shape and wavelet transform. J. Vib. Eng. Technol. 12(3): 2865-2875. https://doi.org/10.1007/s42417-023-01019-y

Saadatmorad M, Talookolaei RAJ, Pashaei MH, Khatir S, Wahab MA (2022) Pearson correlation and discrete wavelet transform for crack identification in steel beams. Math. 10(15): 2689. https://doi.org/10.3390/math10152689

Seguini M, Djamel N, Djilali B, Khatir S, Wahab MA (2022) Crack prediction in beam-like structure using ANN based on frequency analysis. Frat. Integrita. Strutt. 16(59): 18-34. https://doi.org/10.3221/IGF-ESIS.59.02

Sha G, Radzieński M, Cao M, Ostachowicz W (2019) A novel method for single and multiple damage detection in beams using relative natural frequency changes. Mech. Syst. Signal Process. 132: 335-352. https://doi.org/10.1016/j.ymssp.2019.06.027

Song Z, Qi X, Liu Z, Ma H (2018) Experimental study of guided wave propagation and damage detection in large diameter pipe filled by different fluids. NDT & E International 93: 78-85. https://doi.org/10.1016/j.ndteint.2017.10.002

Sotoudehnia E, Shahabian F, Sani AA (2019) A new method for damage detection of fluid-structure systems based on model updating strategy and incomplete modal data. Ocean Eng. 187: 106200. https://doi.org/10.1016/j.oceaneng.2019.106200

Tahir SI, Tounsi A, Chikh A, Al-Osta MA, Al-Dulaijan SU, Al-Zahrani MM (2022) The effect of three-variable viscoelastic foundation on the wave propagation in functionally graded sandwich plates via a simple quasi-3D HSDT. Steel Compos. Struct. Int. J. 42(4): 501-511. https://doi.org/10.12989/scs.2022.42.4.501

Thomson WT (1993) Theory of vibration with applications. NASA STI/Recon Technical Report A. 93: 39794. https://doi.org/10.1201/9780203718841

Tijsseling AS (1996) Fluid-structure interaction in liquid-filled pipe systems: a review. J. Fluids Struct. 10(2): 109-146. https://doi.org/10.1006/jfls.1996.0009

Tounsi A, Bousahla AA, Tahir SI, Mostefa AH, Bourada F, Al-Osta MA, Tounsi A (2024) Influences of different boundary conditions and hygro-thermal environment on the free vibration responses of FGM sandwich plates resting on viscoelastic foundation. Int. J. Struct. Stab. Dyn. 24(11): 2450117. https://doi.org/10.1142/S0219455424501177

Tounsi A, Mostefa AH, Attia A, Bousahla AA, Bourada F, Tounsi A, Al-Osta MA (2023a) Free vibration investigation of functionally graded plates with temperature dependent properties resting on a viscoelastic foundation. Struct. Eng. Mech. 86(1): 1-16. https://doi.org/10.12989/sem.2023.86.1.001

Tounsi A, Mostefa AH, Bousahla AA, Tounsi A, Ghazwani MH, Bourada F, Bouhadra A (2023b) Thermodynamical bending analysis of P-FG sandwich plates resting on nonlinear visco-

Pasternak's elastic foundations. Steel Compos. Struct. 49(3): 307-323. https://doi.org/10.12989/scs.2023.49.3.307

Vassilev VM, Djondjorov PA (2006) Dynamic stability of viscoelastic pipes on elastic foundations of variable modulus. J. Sound Vib. 297(1-2): 414-419. https://doi.org/10.1016/j. jsv. 2006. 03.025

Wahab MA, De Roeck G (1999) Damage detection in bridges using modal curvatures: application to a real damage scenario. J. Sound Vib. 226(2): 217-235. https://doi.org/10.1006/jsvi.1999.2295

Wang F (2018) Effective design of submarine pipe-in-pipe using finite element analysis. Ocean Eng. 153: 23-32. https://doi.org/10.1016/j.oceaneng.2018.01.095

Wang H, Sun D (2019) The application of matching pursuit based on multi feature pattern set in the signal processing of rotating machinery. J. Vib. Control. 25(13): 1974-1987. https://doi.org/10.1177/107754631984443

Yang Z, Wang L (2010) Structural damage detection by changes in natural frequencies. J. Intell. Mater. Syst. Struct. 21(3): 309-319. https://doi.org/10.1016/S0141-0296(96)00149-6

Yu H, Cai C, Yuan Y, Jia M (2017) Analytical solutions for Euler-Bernoulli Beam on Pasternak foundation subjected to arbitrary dynamic loads. Int. J. Numer. Anal. Methods. 41(8): 1125-1137. https://doi.org/10.1002/nag.2672

Zaitoun MW, Chikh A, Tounsi A, Sharif A, Al-Osta MA, Al-Dulaijan SU, Al-Zahrani MM (2023) An efficient computational model for vibration behavior of a functionally graded sandwich plate in a hygrothermal environment with viscoelastic foundation effects. Eng. Comput. 39(2): 1127-1141. https://doi. org/10.1007/s00366-021-01498-1

Zhai HB, Wu ZY, Liu YS, Yue ZF (2011) Dynamic response of pipeline conveying fluid to random excitation. Nucl. Eng. Des, 241(8): 2744-2749. https://doi.org/10.1016/j.nucengdes.2011.06.024

Zhang YL, Reese JM, Gorman DG (2002) Finite element analysis of the vibratory characteristics of cylindrical shells conveying fluid. Comput. Methods. Appl. Mech. Eng. 191(45): 5207-5231. https://doi.org/10.1016/S0045-7825(02)00456-5